Molecular Therapy
Oncolytics
Original Article

ROS/KRAS/AMPK Signaling Contributes to Gemcitabine-Induced Stem-like Cell Properties in Pancreatic Cancer

Hengqiang Zhao,[1,3,5] Shihong Wu,[1,2,5] Hehe Li,[1,2] Qingke Duan,[1,2] Zhengle Zhang,[1,2] Qiang Shen,[4] Chunyou Wang,[1,2] and Tao Yin[1,2]

[1]Department of Pancreatic Surgery, Union Hospital, Tongji Medical College, Huazhong University of Science and Technology, Wuhan 430022, China; [2]Sino-German Laboratory of Personalized Medicine for Pancreatic Cancer, Union Hospital, Tongji Medical College, Huazhong University of Science and Technology, Wuhan 430022 China; [3]Department of Breast and Thyroid Surgery, Renmin Hospital of Wuhan University, Wuhan 430060, China; [4]Department of Clinical Cancer Prevention, The University of Texas MD Anderson Cancer Center, Houston, TX 77030, USA

Poor prognosis in pancreatic cancer (PanCa) is partially due to chemoresistance to gemcitabine (GEM). Glucose metabolism has been revealed to contribute to the therapeutic resistance and pluripotent state of PanCa cells. However, few studies have focused on the effects of GEM on cancer cell metabolism, stemness of tumor cells, and molecular mechanisms that critically influence PanCa treatment. We demonstrate that GEM treatment induces metabolic reprogramming, reducing mitochondrial oxidation and upregulating aerobic glycolysis, and promotes stem-like behaviors in cancer cells. Inhibiting aerobic glycolysis suppresses cancer cell stemness and strengthens GEM's cytotoxicity. GEM-induced metabolic reprogramming is *KRAS* dependent, as knockdown of *KRAS* reverses the metabolic shift. GEM-induced metabolic reprogramming also activates AMP-activated protein kinase (AMPK), which promotes glycolytic flux and cancer stemness. In addition, GEM-induced reactive oxygen species (ROS) activate the KRAS/AMPK pathway. This effect was validated by introducing exogenous hydrogen peroxide (H_2O_2). Taken together, these findings reveal a counterproductive GEM effect during PanCa treatment. Regulating cellular redox, targeting KRAS/AMPK signaling, or reversing metabolic reprogramming might be effective approaches to eliminate cancer stem cells (CSCs) and enhance chemosensitivity to GEM to improve the prognosis of PanCa patients.

INTRODUCTION

Cytotoxic chemotherapy with gemcitabine (GEM) continues to be the first-line treatment for pancreatic cancer (PanCa). However, GEM treatment has been minimally effective at the improving the prognosis of PanCa patients.[1] One of the speculative causes of this limited effectiveness has been the postulated existence of relatively rare but highly chemoresistant cancer stem cells (CSCs).[2,3] CSCs have been reported to possess inherently high tumor-initiating potential, which is implicated in tumor relapse, as well as in establishment of metastases.[4,5]

Accumulating evidence has shown that resistance of some cancers to chemotherapy may result from dysregulation of glucose metabolism.[6] Tumor cells rewire their metabolic pathways to ensure an energy supply, and as a part of survival programs activated in response to environmental threats.[7] In addition, ionizing radiation has been found to induce metabolic changes that correlate with induction of the CSC phenotype,[8] thus promoting expansion of the CSC-like population and enhancing resistance to anticancer drugs.[9] Elucidation of the effects of GEM on cancer cell metabolism and stemness is expected to contribute to our understanding of the underlying mechanism(s) of chemoresistance in PanCa cells.

Accumulating evidence suggests that PanCa cells' metabolic switch ability is regulated by various oncogenic signals.[10] Oncogenic *KRAS* mutations function as a key driver in initiation and maintenance of approximately 90% of PanCa cases.[11] The *KRAS* oncogene encodes a small GTPase (21 kDa), which is active in its GTP-bound form and inactive when bound to GDP.[11] Aberrant KRAS activation can cause dysfunction in oxidative phosphorylation (OXPHOS). Compensatory elevated aerobic glycolysis can drive tumor development.[12–14] With *KRAS* ablation, surviving tumor cells experience impaired aerobic glycolysis, have increased mitochondrial activity, and rely largely on OXPHOS for energy. At the same time, AMP-activated protein kinase (AMPK) phosphorylation is lower in *KRAS*-ablated tumor cells than in *KRAS*-expressing cells.[15] The transition from OXPHOS to aerobic glycolysis is a prerequisite to the reprogramming of differentiated cells to a pluripotent state.[16] Such a transition in cellular metabolism could cause an energy crisis. To restore an adequate energy supply, AMPK, a key regulator of cellular energy

Received 22 June 2019; accepted 23 July 2019;
https://doi.org/10.1016/j.omto.2019.07.005.

[5]These authors contributed equally to this work.

Correspondence: Tao Yin, Department of Pancreatic Surgery, Union Hospital, Tongji Medical College, Huazhong University of Science and Technology, Wuhan 430022, China.
E-mail: ytwhun@hust.edu.cn

metabolism, stimulates ATP generation by promoting glucose uptake and transport.[17] In addition to acting as a stress-response molecule, AMPK is associated with drug resistance and enrichment of CSCs.[18] Increased levels of reactive oxygen species (ROS) upon GEM treatment have been reported previously.[19,20] Multiple studies have shown that high ROS levels are cytotoxic and low ROS levels may be tumor promoting.[20,21] In this study, we demonstrated that low-dose GEM can induce metabolic reprogramming toward aerobic glycolysis, promoting PanCa cell stem-like properties and chemoresistance. Mechanistically, GEM-induced metabolic reprogramming and cancer stemness are regulated by ROS-mediated activation of the KRAS/AMPK pathway. These findings may shed light on how GEM induces therapeutic resistance and provide novel potential approaches for better management of PanCa.

RESULTS

GEM Treatment Induces Metabolic Reprogramming of PanCa Cells toward Dependence on Aerobic Glycolysis

Recently, we demonstrated that GEM-resistant PanCa cells underwent a metabolic shift, becoming more glycolytic.[22] However, it remains unclear whether this metabolic reprogramming is induced by GEM treatment. We first examined the effect of GEM on expression of glycolytic genes. GEM treatment increased the mRNA expression in PanCa cells of many glycolytic enzymes reported to contribute to tumor aggressiveness or drug resistance in cancer cells; these include *GLUT1*, *HKII*, *PFKP*, *ALDOA*, *TPI1*, *PGK1*, *PGAM1*, *PKM2*, and *LDHA* (Figure S1A).

We utilized 2-(N-(7-nitrobenz-2-oxa-1,3-diazol-4-yl)amino)-2-deoxyglucose (2-NBDG), a fluorescent deoxyglucose analog, to monitor glucose uptake and found that GEM treatment increased 2-NBDG uptake in PanCa cells (Figure 1A). In addition, after GEM treatment, the lactate concentration in the culture medium increased dramatically, indicating increased conversion of pyruvate to lactate (Figure 1B). Importantly, when 2-deoxy-D-glucose (2-DG)—a glucose analog that competes with glucose for uptake via GLUT1, is phosphorylated by HKII, and allosterically inhibits HKII, thus functioning as a glycolysis inhibitor—was introduced,[23] GEM-induced elevation in lactate production was significantly reduced (Figure 1C). Similarly, GEM dose-dependently upregulated protein and mRNA levels of glucose transporter 1 (GLUT1), which is responsible for uptake of extracellular glucose and lactate dehydrogenase A (LDHA), an enzyme responsible for conversion of pyruvate into lactate (Figure 1D). Taken together, high glucose uptake and lactate production suggest that glycolysis was upregulated upon GEM treatment.

At the intersection of aerobic glycolysis and respiration, pyruvate dehydrogenase kinase (PDK)—which inhibits pyruvate dehydrogenase (PDH) and prevents entry of pyruvate into OXPHOS-based metabolism—plays a key role in cellular glucose metabolism. Interestingly, we detected four genes encoding kinases (*PDK1*, *PDK2*, *PDK3*, and *PDK4*) that inhibit PDH enzyme complex activity and found that *PDK2* was significantly induced at the mRNA level in all three cell lines treated with GEM (Figure S1B). We therefore examined protein levels of PDK2. As expected, GEM dose-dependently upregulated expression of PDK2 protein (Figure 1E). Similarly, GEM significantly increased levels of phospho-PDHE1-α (Ser 293) (p-PDHE1-α) in a dose-dependent manner (Figure 1E). PDK phosphorylates the PDHE1-α subunit, and inactivates the PDH enzyme complex that converts pyruvate to acetyl-coenzyme A, thereby inhibiting pyruvate metabolism via the tricarboxylic acid (TCA) cycle. In addition, mitochondrial membrane potential ($\Delta\Psi m$) is generated by OXPHOS activity. Thus, a decrease in $\Delta\Psi m$ is indicative of decreased electron transport and OXPHOS activity.[24] We observed that GEM treatment decreased $\Delta\Psi m$ (Figure 1F) without affecting cell viability (Figure S2A). These findings suggest that GEM treatment induces metabolic reprogramming.

Inhibition of Aerobic Glycolysis Abrogates GEM-Induced Enhancement of Cancer Stemness

We first investigated the cancer stem-like properties of GEM-treated PanCa cells. CSCs are defined by their ability to form tumor spheres in culture, under non-adherent conditions.[3,25] PanCa cells treated with a sub-lethal dose of GEM (Figure S2A) exhibited an enhanced ability to form tumor spheres in ultra-low adhesion plates (Figure S2B). We also found that the mRNA and protein expression levels of the pluripotent cell markers Nanog and Sox2[25] increased in cells treated with GEM in a dose-dependent manner (Figure S2C). We further found that GEM significantly increased expression of *ALDH*, *OCT4*, *KLF4*, *CXCR4*, and *CD24*, which have previously been reported to be CSC markers in all three cell lines,[3,26–28] and *EPCAM*, which has been reported to be a CSC marker in SW1990 cells (Figure S2D). GEM-mediated upregulation of *ABCG2* and *MDR1* levels has been associated with drug resistance (Figure S2E).[29] In addition, *ID-1*, *MUC-1*, and *MUC-4* expression is upregulated upon GEM treatment, indicating decreased differentiation (Figure S2F).[30,31] Furthermore, GEM dose-dependently increased expression of epithelial-mesenchymal transition (EMT)-associated genes, such as *N-cadherin*, *Vimentin*, *Snail1*, and *Zeb1*, in PanCa cells (Figure S2G).[32]

We further investigated whether inhibition of aerobic glycolysis could abrogate GEM-induced PanCa cell stemness. We found that 2-DG, a glycolytic inhibitor, partially abrogated GEM-induced expression of Nanog and Sox2 at protein and mRNA levels (Figures 2A and 2B). To confirm that the enhanced cancer cell stemness induced by GEM was glycolysis-dependent, we examined the expression of CD133, a CSC surface marker on PanCa cells.[25,28,32,33] Treatment with 2-DG significantly decreased GEM-induced CD133 expression (Figures 2C and 2D). Treatment of Patu8988 cells with a nontoxic low dose of 2-DG (5 mM, 24 h) suppressed sphere formation (Figures S2A and S2H). 2-DG significantly reinforced GEM cytotoxicity in PanCa cells, significantly decreasing its lethal dose 50% (LD_{50}) in PanCa cells (Figures 2E and 2F). Thus, inhibition of glycolysis suppressed GEM-induced stemness and enhanced the therapeutic efficacy of GEM in PanCa cells.

We further detected the involvement of glycolysis in tumorigenesis of pancreatic cancer cells treated with GEM (Figure 3A). As shown in

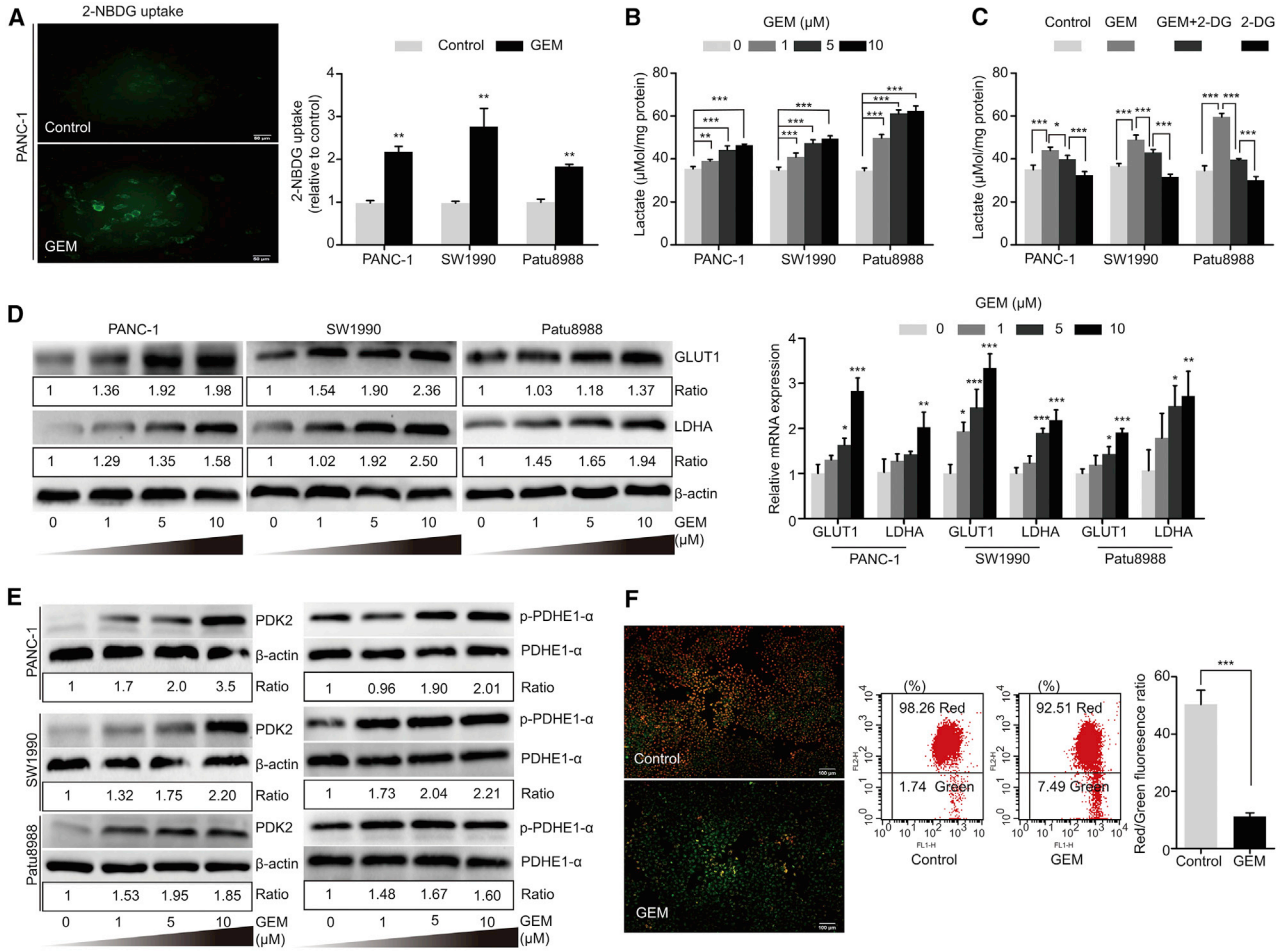

Figure 1. GEM Induces Metabolic Reprogramming Favoring Aerobic Glycolysis in PanCa Cells

(A) Uptake of the glucose analog 2-NBDG was measured in PANC-1, SW1990, and Patu8988 cells treated with GEM (5 μM, 24 h) or vehicle. Representative images of 2-NBDG uptake in PANC-1 cells captured by fluorescence microscopy (left) and quantification of uptake by flow cytometry (right). Scale bar, 50 μm. (B) Extracellular lactate was measured following 36 h of exposure to different doses of GEM. (C) Effect of 2-DG on GEM-induced lactate production. All three cell types were pretreated with 2-DG (5 mM, 1 h) followed by treatment with GEM. (D) GEM dose-dependently upregulated expression of GLUT1 and LDHA at both protein and mRNA levels. All three cell lines were treated with increasing concentrations of GEM for 24 h. Total protein and RNA were extracted for western blot and qRT-PCR analyses, respectively. Ratios are expressed as fold change relative to control values, which are normalized to 1 after being normalized against β-actin. (E) Western blot analyses showed increasing expression of PDK2 and p-PDHE1-α. Cells were treated as indicated in (D). Ratios represent the intensity of bands of PDK2 or p-PDHE1-α normalized against β-actin or total PDHE1-α, respectively, then normalized against controls. Densitometry was performed by Image Lab software. (F) $\Delta\Psi$m in PANC-1 cells treated with GEM (5 μM, 24 h) determined by the JC-1 method. GEM treatment depolarized $\Delta\Psi$m, causing more green than red JC-1 fluorescence. Representative images of fluorescence microscopy (left), flow cytometry analysis (middle), and quantification (right) are shown. Scale bar, 100 μm. GEM, gemcitabine. Data shown are from three independent experiments. Error bars represent means ± SD. β-actin served as an internal control. *$p < 0.05$, **$p < 0.01$, ***$p < 0.001$.

Figures 3B and 3C, pretreatment of pancreatic cancer cells (SW1990) with a sub-lethal dose of GEM increased the tumor growth rate and cell size of SW1990 cell xenografts in mouse models compared with controls. Remarkably, 2-DG inhibited the growth-promoting effects of GEM pretreatment on pancreatic cancer cells. These results are in agreement with the abrogation of GEM-induced stemness by inhibiting glycolysis. To verify whether tumorigenesis in different treated groups correlated with stemness, we performed CD133, Nanog, and Sox2 immunostaining. As shown in Figure 3E, levels of stemness markers, including CD133, Nanog, and Sox2, increased in the GEM treated group but were abrogated in cells also treated with 2-DG.

Oncogenic *KRAS* Is Involved in GEM-Induced Metabolic Reprogramming and Cancer Cell Stemness

It has already been reported that *KRAS* (G12V) transformation leads to mitochondrial dysfunction and metabolic switching.[12] We therefore investigated the role of *KRAS* in GEM-induced metabolic reprogramming. We first evaluated the effect of GEM on KRAS activation. As revealed in Figure 4A, GEM exposure effectively activated KRAS,

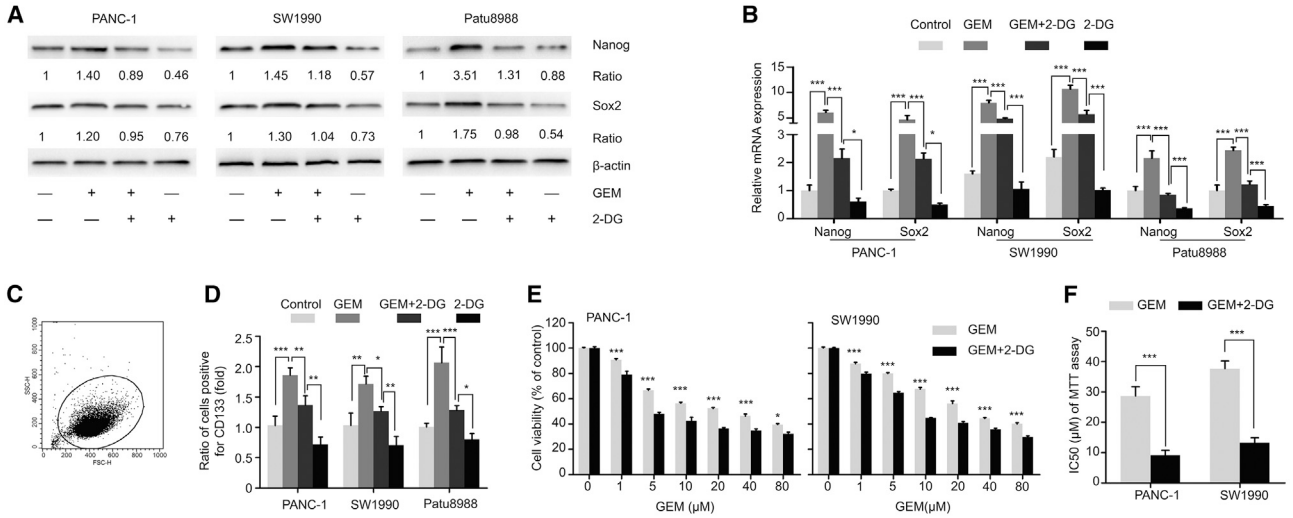

Figure 2. GEM-Induced Cancer Cell Stemness Is Abrogated by Inhibition of Aerobic Glycolysis

(A and B) Inhibition of the pluripotency markers Nanog and Sox2, following 2-DG treatment. PANC-1, SW1990, and Patu8988 cells were pretreated with 2-DG (5 mM, 1 h) followed by GEM treatment for 24 h. Total protein and RNA were extracted for western blot (A) and qRT-PCR (B) analyses, respectively. Ratios are expressed as fold change compared with control values, normalized to 1 after being normalized against β-actin. β-actin served as an internal control. (C and D) Flow cytometry analysis of the CSC cell surface marker, CD133. Representative images of the gating strategy for PANC-1 cells (C) and quantification of the assay (D). (E and F) PANC-1 and SW1990 cells were treated with increasing concentrations of GEM ± 2-DG (5 mM) for 48 h. Cell viability was measured using an MTT assay. Representative results (E) and quantification of LD_{50} (F) are shown. All experiments were repeated at least three times. Error bars represent means ± SD. *$p < 0.05$, **$p < 0.01$, ***$p < 0.001$.

producing higher levels of GTP-bound KRAS compared with those in the control group. We assessed the effect of *KRAS* knockdown on metabolic reprogramming. Knockdown of *KRAS* decreased expression of most glycolytic genes (Figures S3A and S3B). Importantly, knockdown of *KRAS* reduced lactate production (Figure 4B), suppressed expression of PDK2, and consequently decreased p-PDHE1-α levels (Figure 4C), indicating restoration of OXPHOS. In addition, $\Delta\Psi m$ was not decreased upon *KRAS* knockdown, as revealed by fluorescence microscopy and flow cytometry analyses (Figure 4D). Maintenance of $\Delta\Psi m$ indicates functional OXPHOS. These results suggest that activation of KRAS can inhibit mitochondrial function and drive the metabolic switch to aerobic glycolysis.

We further assessed the role of *KRAS* in maintenance of cancer stemness and chemoresistance. *KRAS* knockdown decreased sphere formation ability (Figure 4E) and expression of pluripotent markers (Figures 4F and 4G). In addition, *KRAS* knockdown significantly enhanced the cytotoxicity of GEM, 2-DG, or both, as demonstrated by decreased LD_{50} (Figure 4H). Taken together, these results establish that the metabolic switch from aerobic glycolysis to OXPHOS, induced by *KRAS* knockdown, inhibited cancer stemness and sensitized PanCa cells to chemotherapeutics.

The role of KRAS in GEM-induced metabolic reprogramming and cancer cell stemness was further assessed *in vivo* (Figure 5A). A pancreatic cancer xenograft model was established by subcutaneous injection of pancreatic cancer cells into the right flank of nude mice. Treatments were initiated after comparable tumor volumes were reached in tumor-bearing mice (approximately 100 mm^3) as described in the Supplemental Materials and Methods. The role of KRAS was assessed by local injection of cholesterol-conjugated KRAS small interfering RNA (siRNA) into the tumor mass. The efficacy of KRAS siRNA transfection *in vivo* was evaluated by immunohistochemically analyzing KRAS expression in tumor tissue. While the growth rate and final size of tumors in the GEM chemotherapy group were slightly, but not dramatically, reduced compared with that in the NC siRNA group, KRAS siRNA alone substantially decreased tumor growth. GEM combined with KRAS siRNA significantly decreased the tumor's growth compared with GEM chemotherapy alone (Figures 5B–5D). KRAS expression was significantly downregulated in GEM-treated and -untreated groups after KRAS siRNA transfection (Figure 5E). Immunohistochemical staining of glycolytic enzymes, including GLUT1, LDHA, HKII, and PDK2, showed enhanced glycolysis in the group treated with gemcitabine, which could be abrogated by *in vivo* silencing of KRAS (Figure 5F). Similarly, GEM-induced enhancement of cancer stemness was reduced by KRAS knockdown *in vivo* (Figure 5G).

GEM-Induced Metabolic Shift Activates AMPK

As observed above, GEM induces a metabolic shift from OXPHOS toward aerobic glycolysis, which is a less efficient pathway to supply cellular energy. AMPK is an evolutionarily conserved energy sensor, modulating cellular energy flux in response to energy crises.[34] We therefore examined the effects of GEM on AMPK activation. As expected, GEM dose-dependently enhanced phosphorylation of AMPKα (Thr172) (p-AMPKα) (Figure 6A), which has been

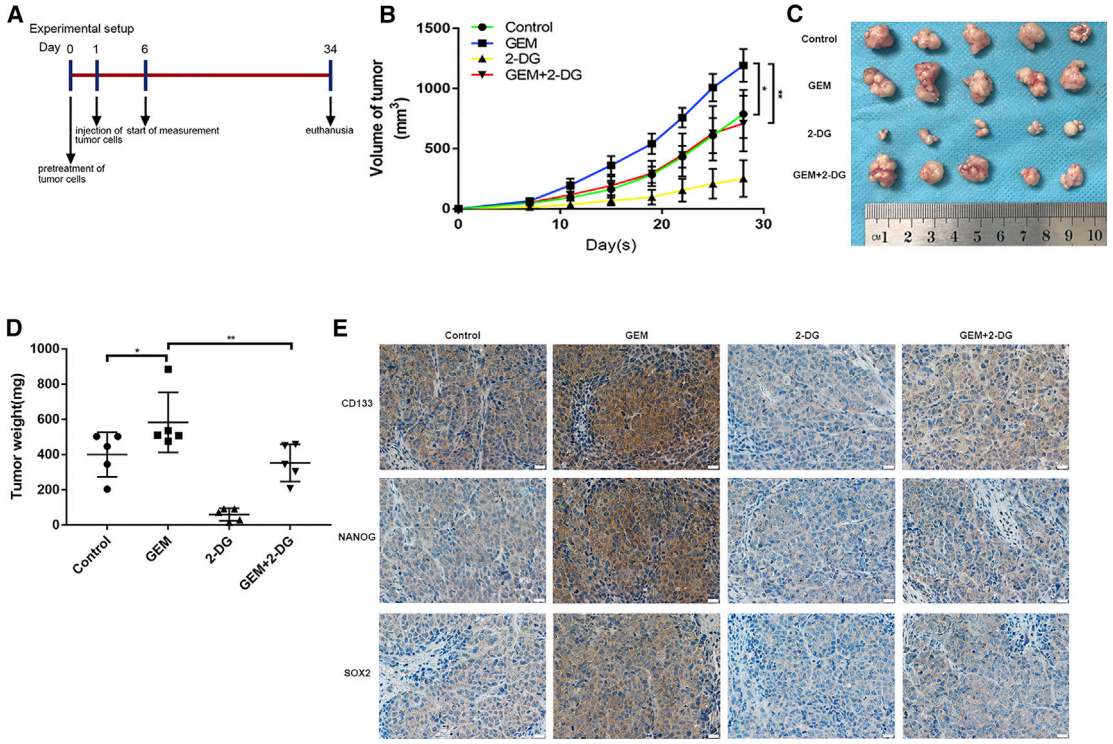

Figure 3. GEM-Induced Cancer Cell Stemness Is Abrogated by Inhibition of Glycolysis *In Vivo*

(A) General experimental setup of the *in vivo* study. (B) Tumor volumes were measured after every 3 days. Tumor growth curves were drawn according to measured tumor volumes. (C) Pretreated SW1990 cells were subcutaneously injected into the right flank of nude mice. Representative images of tumor size at 28 days is shown (n = 5). (D) Tumor weights were measured after harvesting. (E) Representative tumor tissue sections from xenografts in different treatment groups were analyzed by immunohistochemistry for expression of cancer stemness markers, including CD133, NANOG, and SOX2. *p < 0.05, **p < 0.01, ***p < 0.001.

speculated to correlate with enzyme activity.[35] To further examine whether the rewired cellular metabolism activates AMPK, we examined the effect of *KRAS* knockdown on AMPK activation. As expected, knockdown of *KRAS* reduced levels of p-AMPKα (Figure 6B), suggesting a regulatory role of *KRAS*-mediated cellular metabolism in AMPK activation.

AMPK's involvement in the regulation of glycolytic flux is well documented.[36] We therefore investigated whether AMPK is involved in GEM-induced metabolic reprogramming. We pretreated cancer cells with compound C, an inhibitor of AMPK, followed by exposure to GEM. GEM-induced p-AMPKα expression was abrogated by compound C, which showed marginal effect on p-PDHE1-α generation (Figure 6C). Compound C also significantly inhibited GEM-induced lactate production (Figure 6D), suggesting that glycolysis was inhibited. We also observed that PanCa cells treated with compound C exhibited reduced sphere formation (Figure 6E), indicating diminished expression of pluripotency markers (Figure 6F). In addition, compound C strengthened the cytotoxicity of GEM toward PanCa cells, resulting in a decreased LD_{50} (Figures 6G and 2F).

To further investigate the potential role of AMPK in glycolytic flux, we introduced a selective AMPK activator, A-769662. Treatment with A-769662 led to AMPK activation but did not exhibit a significant effect on p-PDHE1-α levels (Figure S4A). We did not observe a significant difference in lactate production after A-769662 treatment (data not shown). However, A-769662 treatment promoted expression of glycolytic genes, such as GLUT1 and LDHA (Figure S4B). Unlike compound C, A-769662 promoted sphere formation, pluripotent cell marker expression, and tumor cell viability at appropriate concentrations (Figures S4C–S4E). Taken together, these findings demonstrate that AMPK mediates GEM-induced upregulation of aerobic glycolysis and promotes reacquisition of cancer cell stemness.

GEM-Induced ROS Participates in Activation of the KRAS/AMPK Pathway, Metabolic Reprogramming, and Cancer Stemness

Induction of ROS upon GEM treatment has been previously reported.[19,20] To examine whether GEM-induced ROS activates the KRAS/AMPK pathway, we first examined ROS production upon GEM treatment. Consistent with previous findings, GEM treatment induced a dose-dependent increase in ROS levels, which was abrogated by introduction of N-acetyl-cysteine (NAC) (a free-radical scavenger) (Figure 7A). Importantly, GEM-induced upregulation of both KRAS-GTP and p-AMPKα was abrogated by pretreatment with NAC (Figure 7B). Next, we found that GEM-induced lactate production was reduced (Figure 7C) and p-PDHE1-α expression

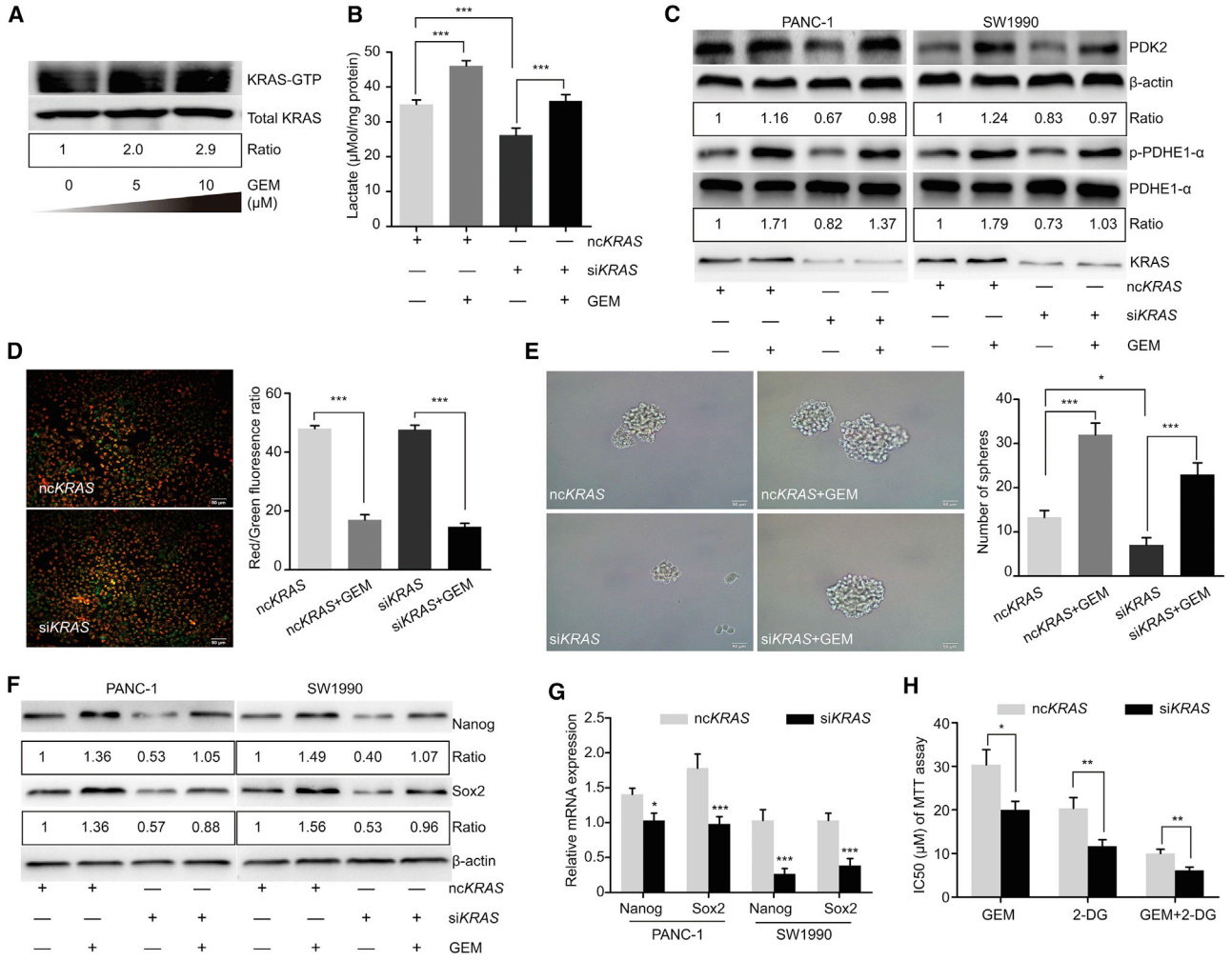

Figure 4. Oncogenic *KRAS* Is Involved in Regulation of GEM-Induced Metabolic Reprogramming and Cancer Cell Stemness

(A) Effect of GEM treatment on KRAS activation. PANC-1 cells were treated with GEM for 24 h. Activation of KRAS was analyzed as described in Materials and Methods. Ratios represent the intensity of the KRAS-GTP band normalized against total KRAS and then normalized against control. (B) Knockdown of *KRAS* inhibited lactate production in PANC-1 cells. Cells were first transfected with si*KRAS* or nc*KRAS*. Following 48 h of transfection, cells were treated with GEM (5 μM) or vehicle for 24 h. (C) *KRAS* knockdown inhibited expression of PDK2 and activation of PDHE1-α. Cells were treated as in (B). Ratios represent the intensity of the pPDHE1-α band normalized against total PDHE1-α, then normalized against control. (D) Role of *KRAS* in regulation of $\Delta\Psi$m. PANC-1 cells were treated as indicated. $\Delta\Psi$m was assessed using fluorescent microscopy (left) and quantified (right). Cells with *KRAS* knockdown showed comparable fluorescence to that of control cells. (E) Knockdown of *KRAS* inhibited sphere formation in PANC-1 cells. Cells were treated as indicated and cultured as described in Materials and Methods. (F) Effect of *KRAS* knockdown on Nanog and Sox2 expression in PANC-1 and SW1990 cells. Ratios are expressed as fold change compared with control values, which are normalized to 1 after being normalized against β-actin. (G) PANC-1 and SW1990 cells were transfected with siRNA targeting *KRAS*, as indicated. Analysis of qRT-PCR was used to examine expression of Nanog and Sox2 mRNA. (H) Effect of *KRAS* knockdown on cell viability. PANC-1 cells were plated in 96-well plates and transfected with si*KRAS*. After transfection, cells were treated with increasing concentrations of GEM (as indicated), 2-DG (0, 1, 5, 10, 20, 40, and 80 mM), or increasing GEM and 2-DG (5 mM) for 48 h. Cell viability was analyzed using an MTT assay and reported as LD_{50}. All experiments were repeated at least three times. Error bars represent means ± SD. β-actin served as an internal control. *$p < 0.05$, **$p < 0.01$, ***$p < 0.001$.

was diminished by NAC treatment (Figure 7D), indicating that GEM-induced activation of KRAS/AMPK signaling was ROS-dependent.

We further found that GEM-induced sphere formation (Figure 7E), CD133 expression (Figure 7F), and pluripotency markers (Figures 7G and 7H) were all inhibited by pretreatment with NAC. To avoid ROS-induced oxidative damage, cancer cells often upregulate their antioxidant production capacity. We observed a significant increase in the expression of antioxidant genes, such as superoxide dismutase 1 (*SOD1*), superoxide dismutase 2 (*SOD2*), catalase (*CAT*), glutathione peroxidase 1 (*GPX1*), and nuclear factor (erythroid-derived 2)-like 2 (*Nrf2*), in PanCa cells (Figure S5), suggesting that

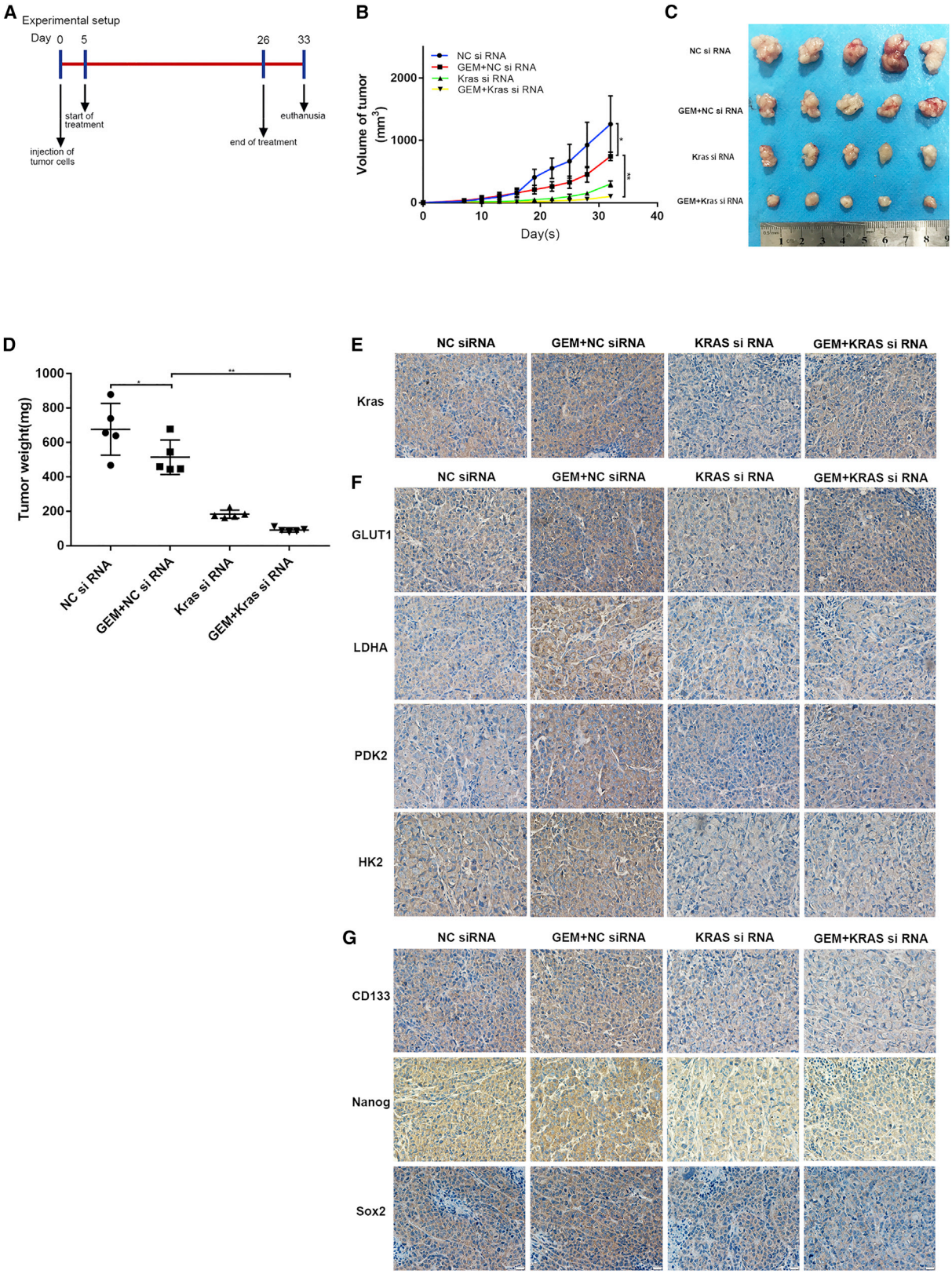

(legend on next page)

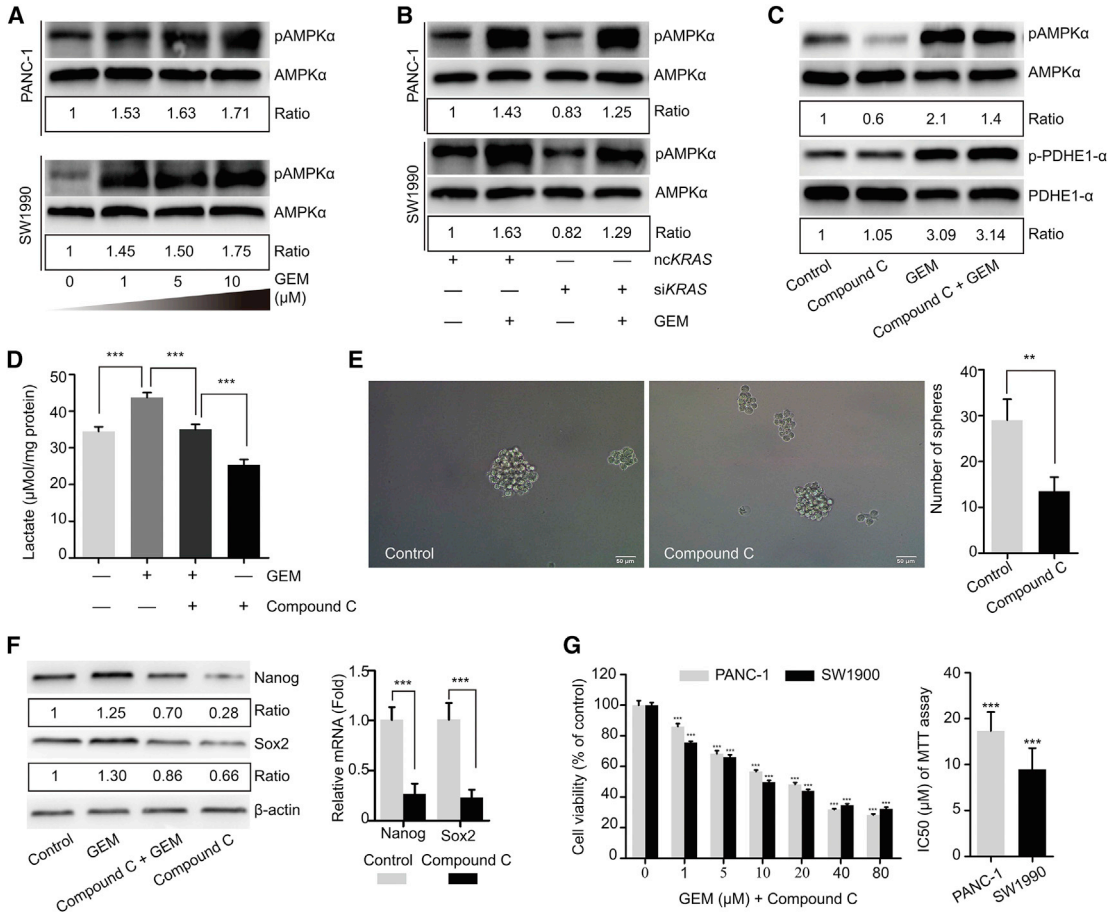

Figure 6. GEM-Induced Metabolic Shift Activates AMPK

(A) AMPK activation was examined by western blot in PANC-1 and SW1990 cells treated as indicated. (B) GEM-induced activation of AMPK was reversed by *KRAS* knockdown. PANC-1 and SW1990 cells were treated as in Figure 3C. (C) Effect of AMPK inhibitor compound C on p-AMPKα and p-PDHE1-α. PANC-1 cells were pretreated with 1 μM compound C for 1 h followed by treatment with 5 μM GEM for 24 h. (D) Compound C inhibited GEM-induced lactate production. PANC-1 cells were pretreated with 1 μM compound C for 1 h followed by treatment with GEM (5 μM) for 36 h. (E) Compound C inhibited sphere formation ability in PANC-1 cells. PANC-1 cells were treated with compound C (1 μM, 24 h). Treated cells (1×10^4 cells) were cultured as indicated for sphere formation. (F) Compound C suppressed expression of Nanog and Sox2 at both protein and mRNA levels. PANC-1 cells were treated as in (C) for western blot or as in (E) for qRT-PCR analysis. Ratios were obtained as previously described. (G) PANC-1 and SW1990 cells were treated with increasing concentrations of GEM combined with compound C (1 μM) for 48 h. MTT assays were used to assess cell viability. β-actin served as an internal control. All experiments were repeated at least three times. Error bars represent means ± SD. Ratios represent the intensity of band of p-AMPKα or p-PDHE1-α normalized against total AMPKα or PDHE1-α, respectively, then normalized against control. **p < 0.01, ***p < 0.001.

GEM-induced oxidative stress is accompanied by an increase in antioxidant reactions.

To further establish the role of oxidative stress in activation of the KRAS/AMPK pathway, we introduced exogenous hydrogen peroxide (H_2O_2) to increase ROS levels to a comparable extent to levels induced by GEM in PanCa cells (Figure 8A). Similar to GEM treatment, H_2O_2 induced KRAS/AMPK activation, which was also inhibited by NAC (Figure 8B). In addition, H_2O_2 increased glycolytic gene expression (Figure S6) and lactate production (Figure 8C),

Figure 5. KRAS Knockdown Inhibits GEM-Induced Metabolic Reprogramming and Cancer Cell Stemness *In Vivo*

(A) The general experimental setup of the *in vivo* study. (B) Tumor volumes were measured at the end of every 3 days. Tumor growth curves were drawn according to measured tumor volumes. (C) SW1990 cells were subcutaneously injected into the right flank of nude mice. After about 7 days, when tumor volumes were comparable (approximately 100 mm^3) mice were randomly divided into NC siRNA, GEM + NC siRNA, KRAS siRNA, and GEM + KRAS siRNA groups, and treated as described in Materials and Methods. Representative images of tumor size at 35 days are shown (n = 5). (D) Tumor weights were measured 1 week after the last treatment. (E–G) Representative tumor tissue sections from xenografts in different treatment groups were analyzed by immunohistochemistry for expression of KRAS (E), glycolytic enzymes including GLUT1, LDHA, HKII, and PDK2 (F), and cancer stemness markers, including CD133, NANOG, and SOX2 (G). *p < 0.05, **p < 0.01, ***p < 0.001.

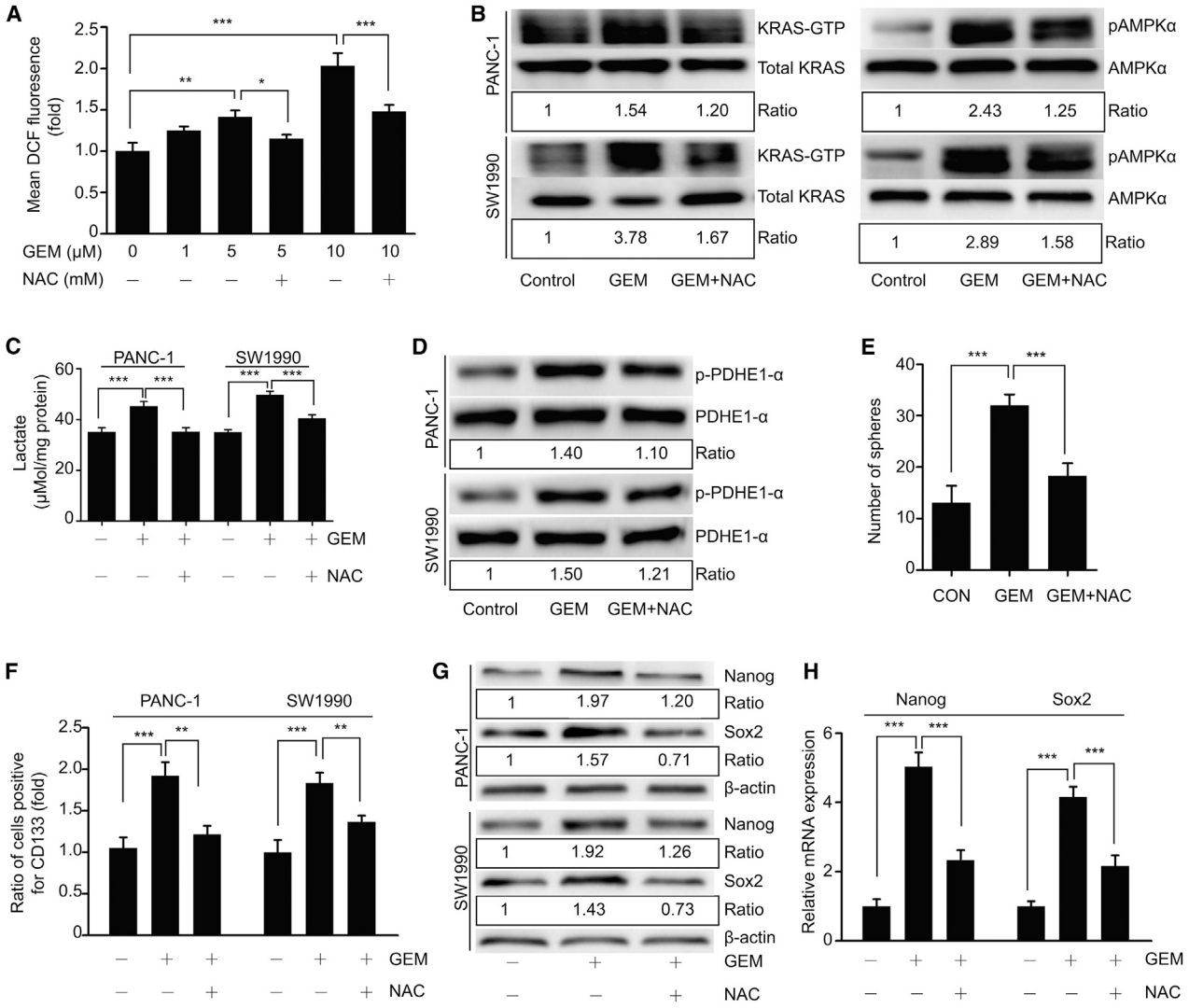

Figure 7. GEM-Induced ROS Is Involved in Activation of the KRAS/AMPK Pathway

(A) ROS levels were measured using flow cytometry with a DCFH-DA probe in PANC-1 cells pretreated with 5 mM NAC (a ROS scavenger) for 1 h followed by treatment with different doses of GEM for 24 h. (B) Role of ROS in activation of the KRAS/AMPK pathway. PANC-1 and SW1990 cells were pretreated with NAC (5 mM, 1 h) followed by treatment with GEM (5 μM) for 24 h. Activation of KRAS and AMPK were evaluated by western blot. (C) Lactate production by PANC-1 and SW1990 cells pretreated with NAC (5 mM, 1 h) followed by treatment with GEM (5 μM) for 36 h. (D) Levels of p-PDHE1-α in cells treated as in (B) were examined by western blot. Ratios represent the intensity of the p-PDHE1-α band normalized against total PDHE1-α, then normalized against the control. (E–H) Effect of GEM-induced ROS on cancer stemness. (E) PANC-1 cells were treated as in (B). Treated cells were cultured as described. (F and G) CD133 and the pluripotency markers Nanog and Sox2 were examined using flow cytometry (F) or western blot (G) in cells treated as in (B). Ratios were obtained as previously described. (H) qRT-PCR analysis was used to examine mRNA levels of Nanog and Sox2 in PANC-1 cells treated as in (B). β-actin served as an internal control. Ratios represent the intensity of the KRAS-GTP or p-AMPKα bands, normalized against total KRAS or AMPKα, then normalized against controls. GEM, gemcitabine. All experiments were repeated at least three times. Error bars represent means ± SD. *$p < 0.05$, **$p < 0.01$, ***$p < 0.001$.

indicating that glycolytic flux was elevated. Importantly, H_2O_2-induced lactate and p-PDHE1-α generation was suppressed following NAC treatment (Figures 8C and 8D). Moreover, H_2O_2-induced sphere formation, CD133 expression, and expression of pluripotency markers were all decreased after treatment with NAC (Figures 8E–8H). Taken together, these findings establish that GEM induces metabolic reprogramming and cancer stemness via ROS-dependent activation of the KRAS/AMPK pathway (Figure 9).

DISCUSSION

Chemoresistance is one of the main causes of poor prognosis in pancreatic cancer. Accumulating evidence suggests that CSCs are resistant to conventional chemotherapy and radiotherapy and may be one of the major causes of cancer recurrence after chemotherapy.[2,3,25,37,38] Therefore, elucidation of the mechanisms underlying chemoresistance and reacquisition of CSC-like properties could shed light on potential therapeutic approaches to improve PanCa

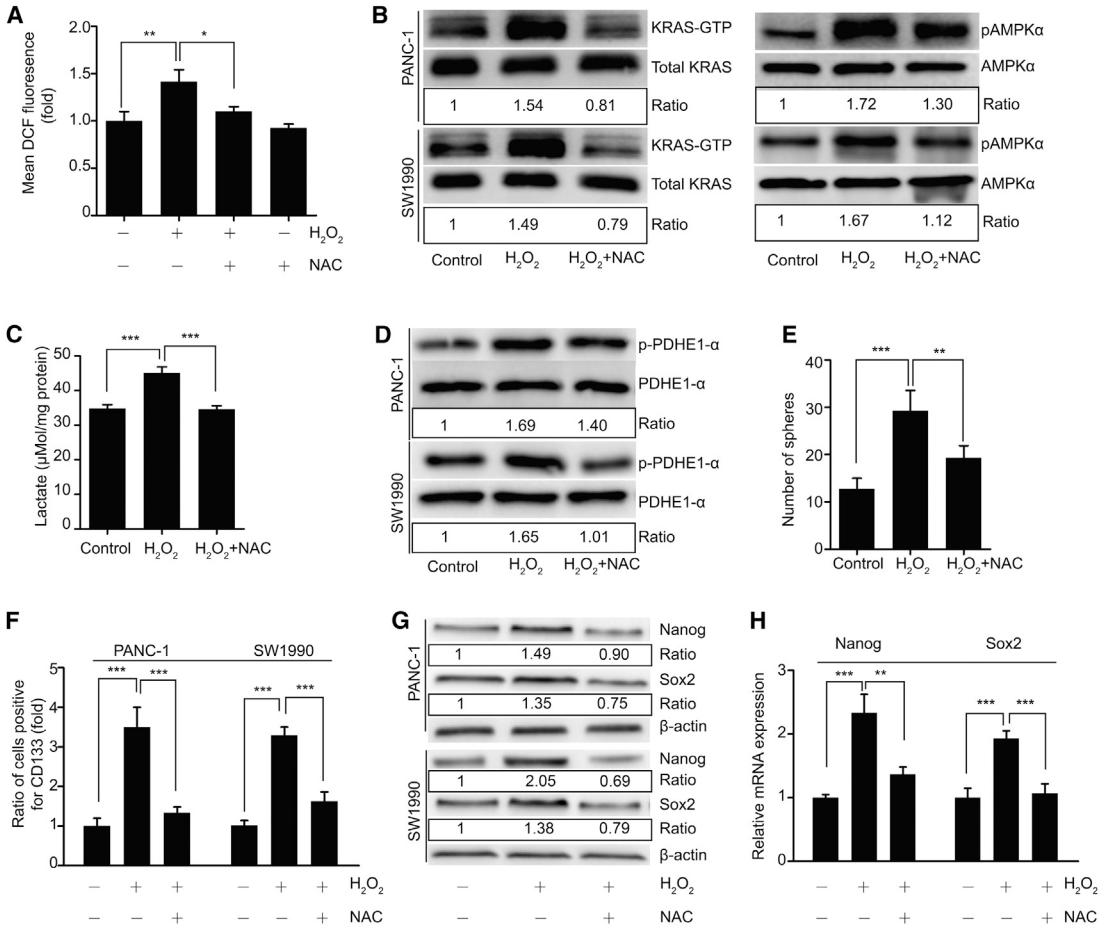

Figure 8. ROS Involvement in Activation of the KRAS/AMPK Pathway

(A) ROS levels in PANC-1 cells pretreated with NAC (5 mM, 1 h), followed by treatment with H_2O_2 (200 μM) for 12 h were assessed using flow cytometry. (B) Activation of the KRAS/AMPK pathway was assessed by western blot. PANC-1 and SW1990 cells were pretreated with NAC (5 mM, 1 h) followed by treatment with H_2O_2 (200 μM) for 24 h. (C) Lactate production in PANC-1 cells pretreated with NAC (5 mM, 1 h) followed by treatment with H_2O_2 (200 μM) for 36 h. (D) Levels of p-PDHE1-α in cells treated as in (B) were examined by western blotting. (E–H) H_2O_2-induced ROS were involved in inducing cancer cell stemness. Cells were treated as in (B). (E) Sphere formation assay of PANC-1 cells is shown. (F and G) CD133 and pluripotency markers Nanog and Sox2 were examined using flow cytometry (F) or western blot (G) in PANC-1 and SW1990 cells treated as in (B). (H) mRNA expression of Nanog and Sox2 in PANC-1 cells treated as in (B). β-actin served as an internal control. Ratios were obtained as previously described. All experiments were repeated at least three times. Error bars represent means ± SD. *$p < 0.05$, **$p < 0.01$, ***$p < 0.001$.

treatment. GEM has been the standard chemotherapy regimen for PanCa patients but has yielded unsatisfactory treatment outcomes.[1] In the present study, to the best of our knowledge, we have demonstrated for the first time that GEM treatment induces metabolic reprogramming toward aerobic glycolysis via ROS-mediated activation of the KRAS/AMPK pathway, enhancing stemness in PanCa cells.

Pluripotent stem cells and embryonic stem cells have been reported to undergo metabolic transition, including upregulation of glycolysis and downregulation of OXPHOS.[16] Similar to these phenomena, we found that GEM induces metabolic reprogramming that enhances aerobic glycolysis and decreases mitochondrial oxidation. This metabolic reprogramming is accompanied by enhanced cancer cell stemness. Enhanced aerobic glycolysis induced by GEM promotes acidification of the microenvironment, partly due to the extrusion of lactic acid, decreasing the cytotoxic efficiency of GEM on PanCa cells.[39] Therefore, safe and efficient inhibition of glycolysis is a promising anticancer therapy, either by itself or in combination with chemotherapy.[40] In our study, inhibition of glycolysis using 2-DG suppresses cancer stemness and strengthens the cytotoxicity of GEM, suggesting a rationale for combining glycolytic inhibitors with conventional chemotherapy for PanCa treatment. In previous clinical studies, 2-DG has been used to treat cancers, such as prostate cancer and glioma.[41,42] Although its use led to adverse effects including fatigue, dizziness, restlessness, and asymptomatic QTc prolongation,[43] clinical trials confirmed that administration of 2-DG alone or combined with other therapies, such as chemotherapy and radiotherapy, was safe and tolerable. These findings led to initiation of several phase

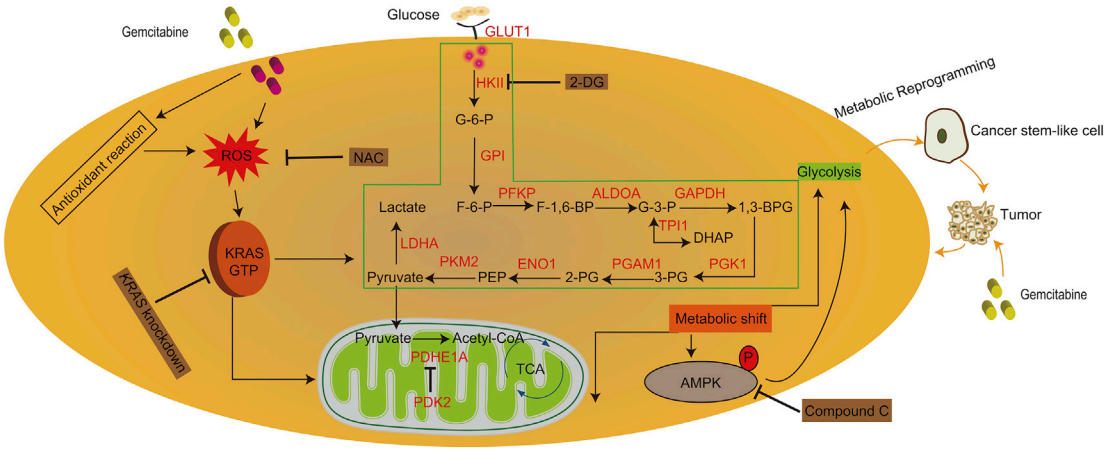

Figure 9. GEM-Induced Activation of the ROS/KRAS/AMPK-Signaling Axis Regulates PanCa Cell Metabolism and Cancer Cell Stemness

GEM treatment induces ROS-mediated, KRAS-dependent metabolic reprogramming from mitochondrial oxidation to aerobic glycolysis, leading to induction of a cancer stem-like cell population, accounting for chemoresistance and tumor recurrence. The metabolic shift is induced by GEM-mediated activation of AMPK, which further promotes glycolysis and cancer stemness. However, the ROS scavenger (NAC), *KRAS* knockdown, an AMPK inhibitor (compound C), or a glycolysis inhibitor (2-DG) can inhibit GEM-induced cancer cell stemness. Abbreviations: see Figure S1A.

II and III clinical trials.[43] Considering the fact that 2-DG can also be taken up by highly metabolic normal tissues, including heart and brain, we must be careful when 2-DG is applied in patients.[39]

Metabolic reprogramming has been recognized as a core hallmark of cancer cells.[44] Oncogenic *KRAS* can produce several phenotypic hallmarks of cancer including altered cellular metabolism.[11] *KRAS* transformation can promote glycolytic activity and decrease oxidative flux.[45] Oncogenic *KRAS* knockdown decreased glucose uptake and lactate production, which demonstrated that oncogenic *KRAS* promotes glycolytic flux in PanCa.[14] Ectopic *KRAS* expression inhibits mitochondrial respiratory chain activity, suppressing mitochondrial respiration.[12] Viale et al. found that surviving cells cultured in semi-solid medium with *KRAS* ablation exhibited decreased aerobic glycolysis and relied on mitochondrial oxidation for survival.[15] Our studies showed that GEM induces KRAS activation, which, in turn, regulates metabolic reprogramming, because knockdown of *KRAS* can inhibit aerobic glycolysis flux and restore mitochondrial respiration. Restoration of cellular metabolism by *KRAS* knockdown suppresses cancer cell stemness and sensitizes PanCa cells to GEM, 2-DG, or both, suggesting a tumorigenic and chemoresistant role for *KRAS*. Similarly, activation of mitochondrial oxidation following PDK2 inhibition could activate mitochondrial apoptotic signaling, causing the death of chemoresistant cancer cells.[46] Mitochondrial OXPHOS is essential for efficient apoptosis.[47,48] The oncogenic role of mutant *KRAS* prompts intensive efforts to explore pharmacological approaches. The association between oncogenic *KRAS* activity and metabolic reprogramming might provide promising directions for the development of novel therapeutic approaches.[11]

It has been reported that GEM-induced ROS is generated by activation of NADPH oxidase (NOX) via nuclear factor κB (NF-κB) activation, as siRNA-mediated depletion of $p22^{-phox}$ (a catalytic subunit of the NOX complex) alleviated GEM-induced ROS production.[20] We also found that GEM-induced ROS was NOX-dependent, because inhibition of NOX using Apocynin (a NOX inhibitor) reduced ROS production.[49] ROS-induced activation of NF-κB can also promote HIF-1α and CXCR4 expression, which play a role in GEM resistance in PanCa cells.[21] Our findings showed that GEM-induced ROS participates in activating the KRAS/AMPK pathway, and this effect can be reversed by pre-treatment with the free-radical scavenger NAC. CSCs reportedly possess mechanisms to fine-tune ROS levels by tightly regulating metabolic pathways such as aerobic glycolysis, rather than by oxidative phosphorylation, to reduce oxidative stress.[50] Nomura et al. found that $CD133^{+}$ pancreatic CSCs showed increased glycolytic flux and decreased mitochondrial activity.[33] This metabolic switch decreased ROS production upon GEM treatment and favored CSC survival. Thus, the metabolic switch induced by GEM is likely a cellular response to oxidative stress, and a prerequisite for induction of CSCs. In addition, GEM-induced expression of antioxidant genes may also play a role in maintenance of intracellular redox homeostasis. GEM treatment increased Nrf2 expression, which regulates production of glutathione (GSH), a major cellular antioxidant that maintains ROS levels within safe parameters to prevent oxidative damage.[20] In addition, ROS-dependent regulation of energy metabolism can drive carbohydrate flux to the pentose phosphate pathway, thereby increasing NADPH levels to counteract intracellular ROS.[51] Cancer cells can rewire metabolic pathways in response to changes in cellular energy and nutrient status, suggesting the complexity of targeting cellular metabolism.

AMPK is a conserved energy sensor and master regulator of cellular metabolism.[34] We found that GEM treatment activates AMPK, probably resulting from the energy crisis induced by GEM treatment, given that restoration of mitochondrial oxidation by *KRAS*

knockdown inhibits AMPK activation. Interestingly, a specific AMPK activator promotes glycolysis, while an AMPK inhibitor inhibits glycolytic flux, suggesting a direct regulatory role of AMPK in glycolysis, consistent with recent findings.[36] AMPK activation may also promote intracellular NADPH production in response to oxidative stress under energy stress conditions.[36,52] AMPK is also critical in modulating self-renewal and chemoresistance of CSCs.[18] We found that AMPK activation promoted glycolysis, cancer cell stemness, and cell survival, suggesting that AMPK inhibition could be a potential means of targeting the malignant behavior of PanCa.

In conclusion, we demonstrated a counterproductive effect of GEM in PanCa treatment. GEM induces KRAS activation, which contributes to metabolic reprogramming and enhances cancer cell stemness. The metabolic shift activates AMPK, which further promotes glycolysis and enhances cancer cell pluripotency. Furthermore, GEM-induced ROS participates in activating KRAS/AMPK signaling, metabolic reprogramming, and maintenance of cancer cell stemness. Considering the implication of metabolic reprogramming in stimulating pluripotency and the contributory role of aerobic glycolysis in chemoresistance, interventions targeting cellular metabolism might provide new therapeutic approaches against PanCa.

MATERIALS AND METHODS

Cell Lines

The human PanCa cell lines PANC-1 and SW1990 were obtained from the American Type Culture Collection (ATCC) (Manassas, USA). Patu8988 cells were obtained from Keygen (KeyGen Biotech, China). All three cell lines harbor a point mutation at codon 12 of the *KRAS* gene (GGT→GAT in PANC-1 and SW1990, and GGT→GTT in Patu8988). Cells were maintained in RPMI Medium 1640 basic (GIBCO by Thermo Fisher Scientific, #8117284) supplemented with 1% penicillin/streptomycin, and 10% fetal bovine serum (GIBCO Invitrogen, Grand Island, NY, USA).

Cell Viability Assay

The effects of various treatments on PanCa cell viability were measured by 3-(4, 5-dimethyl-2-thiazolyl)-2, 5-diphenyl-2H-tetrazolium bromide (MTT) assay as previously described.[22] Pancreatic cancer cell viability was analyzed using an MTT assay (Sigma-Aldrich, #M2128 and #A9251). Cells (PANC-1, SW1900) (6,000 per well) were seeded in 96-well plates overnight. Cells were then treated with different concentrations of gemcitabine (1 to 80 μM) with or without 2-DG (5 mM) for 48 h at 37°C. PANC-1 cells (3×10^3) were seeded and transfected with siRNA-targeting KRAS (siKRAS) or a negative control siRNA (ncKRAS) for 48 h and then treated with GEM (5 μM), 2-DG (5 mM), or their combination for another 36 h. Next, 20 μL of MTT (5 mg/mL in PBS) was added, and cells were incubated for another 4 h. After that, the medium in each well was discarded, and DMSO (Sigma-Aldrich, #D2650) (150 μL) was added. Following agitation for 10 min in the dark on an Eppendorf shaker, absorbance was read at 490 nm in a microplate spectrophotometer. Each concentration was investigated in five replicates. Data were expressed relative to the untreated group.

Western Blot Analysis

Western blots were performed as previously described.[22,49] Cells were lysed with radioimmunoprecipitation assay lysis buffer (Beyotime Biotechnology, Shanghai, China, #P0013C) at 4°C. Equal amounts of protein were separated by 10% SDS-PAGE and transferred to PVDF membranes (Millipore, Billerica, MA, USA, #IPVH00010), which were then blocked with 5% non-fat milk for 1 h and incubated with primary antibodies overnight at 4°C. Membranes were washed and incubated with horseradish peroxidase-coupled secondary antibodies (Aspen, Wuhan, China, #AS1107), and visualized using ECL substrate (Thermo Fisher, Waltham, MA, USA, #32109). Details of various primary antibodies used are provided in the Supplemental Materials and Methods.

Quantitative Real-Time PCR Assay

Total RNA was extracted using TRIzol (Invitrogen, #A33254). Equal amounts of RNA (0.5 μg) were reverse-transcribed to cDNA using PrimeScript RT Master Mix (Takara Bio, #RR036A). Quantitative real-time PCR analysis was performed using a quantitative SYBR Green PCR Kit (Takara Bio, #RR430A), according to the manufacturer's instructions. The data were interpreted with the $2^{-\Delta\Delta CT}$ method, and gene-expression levels were normalized against β-actin levels.

Flow Cytometric Analysis

Mitochondrial membrane potential ($\Delta\Psi m$) of PanCa cells was measured using a mitochondrial membrane potential assay kit with JC-1 (Beyotime, #C2006), according to the manufacturer's instructions. Fluorescence was measured by flow cytometry or fluorescent microscopy. Analysis of the cell surface marker CD133 was performed as previously described.[51]

siRNA-Mediated Knockdown of *KRAS In Vitro* and *In Vivo*

A siRNA sequence targeting the coding region of *KRAS* (si*KRAS*: 5′-GGAAGCAAGTAATTGA-3′) and a nc*KRAS* not matching any human gene sequence were obtained (RiboBio, Guangzhou, China). *KRAS* knockdown was performed by transfecting cells with Lipofectamine 2000 (Invitrogen, #11668019) according to the manufacturer's instructions. Cholesterol-conjugated KRAS siRNA for *in vivo* RNA interference and its negative control were obtained from RiboBio.

Sphere Formation, Glucose Uptake, and Lactate Production Assays

Sphere formation, glucose uptake, and lactate production assays were performed as previously described.[3,22,53] Cells ($5–10 \times 10^3$) subjected to different treatments were cultured in serum-free DMEM-Ham's nutrient mixture (F12) (1:1) medium (Invitrogen) supplemented with 20 ng/mL of epithelial growth factor and 10 ng/mL of basic fibroblast growth factor (PeproTech, #GMP100-15 and #100-25) for 2 weeks. Number of spheres larger than 50 μm was counted using a microscope (Olympus, Tokyo, Japan). For determination of glucose uptake, complete medium was replaced with a glucose-free medium, and cells were incubated for 2 h. Cells were then incubated with the fluorescence-labeled glucose analog 2-NBDG (Cayman Chemical, Ann Arbor, MI, USA) at a final concentration of 10 μM for 30 min at 37°C. Uptake

of 2-NBDG was analyzed using flow cytometry and fluorescence microscopy. To assess lactate production, we cultured cells (3×10^5) overnight. After different treatments, supernatants were collected and centrifuged. Lactate production was assessed using a lactic acid assay kit (Nanjing Jiancheng Bio, Nanjing, China, #A019-2-1) according to the manufacturer's protocol. Lactic acid levels were normalized to total protein in each sample.

Determination of Intracellular ROS Levels

Cells were treated as previously indicated, and incubated with dichlorodihydro-fluorescein diacetate (DCFH-DA) (Beyotime, #S0033) at a final concentration of 10 μM in serum-free medium for 20 min at 37°C.

KRAS Activation Assay

The level of active KRAS was assessed using a RAS activation assay kit (NewEast Biosciences, Malvern, PA, #81101), according to the manufacturer's protocol. Cells were cultured in 10 cm plates to 80%–90% confluence before different treatments. Total cell lysates were collected and incubated with anti-active RAS monoclonal antibody plus protein A/G agarose bead slurry at 4°C for 1 h with gentle agitation. Agarose beads were resuspended in 20 μL of 2× reducing SDS-PAGE sample buffer and boiled. Precipitated active RAS was detected by immunoblot analysis using anti-KRAS monoclonal antibody, according to the manufacturer's instructions.

Tumor Xenografts

All of the procedures involving animals in this study were in accordance with the ethical standards of the Institutional Animal Care and Use Committee of Tongji Medical College, Huazhong University of Science and Technology. Male BALB/c nude mice (5 weeks old) were purchased from HFK Bioscience (Beijing, China). For assessment of glycolysis inhibition on gemcitabine-induced cancer cell stemness *in vivo*, SW1990 cells were pretreated with 5 μM GEM (https://www.selleck.cn; Shanghai, China, #S1714) or 5 mM 2-DG (Sigma-Aldrich, St. Louis, MO, USA, #D8375) or a combination of both for 24 h.

The significance of KRAS inhibition in gemcitabine-induced aerobic glycolysis and cancer stemness in pancreatic cancer *in vivo* was studied by subcutaneous inoculation of cancer cells into nude mice. SW1990 cells (3×10^6/100 μL/mouse) were subcutaneously injected into the right flank of nude mice (n = 5 for each group) followed by treatment with NC siRNA, GEM + NC siRNA, KRAS siRNA, or GEM + KRAS siRNA. Details are provided in Supplemental Materials and Methods.

Immunohistochemistry

Paraffin-embedded xenograft samples were used for immunohistochemical staining of KRAS, cancer stemness markers, including Nanog, Sox2, and CD133, and markers of the cells' glycolysis state, including GLUT1, LDHA, PDK2, and HKII. Details are provided in Supplemental Materials and Methods.

Statistical Analysis

All statistical analyses were performed using GraphPad Prism 5.0 software (San Diego, CA). Unpaired t tests, one-way ANOVA with Bonferroni post-tests, or two-way ANOVA were used to calculate statistical significance. Results were presented as means ± SD. p values < 0.05 were considered statistically significant.

SUPPLEMENTAL INFORMATION

Supplemental Information can be found online at https://doi.org/10.1016/j.omto.2019.07.005.

AUTHOR CONTRIBUTIONS

T.Y. conceived the study. T.Y., H.Z., S.W., and Z.Z. designed the study and wrote the manuscript. H.Z., S.W., H.L., and Q.D. performed the experiments. C.W. and Q.S. provided conceptual advice. Q.S. revised the manuscript.

CONFLICTS OF INTEREST

The authors declare no competing interests.

ACKNOWLEDGMENTS

This work was supported by the National Natural Science Foundation of China (grant numbers 81372665 and 81772564).

REFERENCES

1. de Sousa Cavalcante, L., and Monteiro, G. (2014). Gemcitabine: metabolism and molecular mechanisms of action, sensitivity and chemoresistance in pancreatic cancer. Eur. J. Pharmacol. *741*, 8–16.
2. Gangemi, R., Paleari, L., Orengo, A.M., Cesario, A., Chessa, L., Ferrini, S., and Russo, P. (2009). Cancer stem cells: a new paradigm for understanding tumor growth and progression and drug resistance. Curr. Med. Chem. *16*, 1688–1703.
3. Du, Z., Qin, R., Wei, C., Wang, M., Shi, C., Tian, R., and Peng, C. (2011). Pancreatic cancer cells resistant to chemoradiotherapy rich in "stem-cell-like" tumor cells. Dig. Dis. Sci. *56*, 741–750.
4. Lee, C.J., Dosch, J., and Simeone, D.M. (2008). Pancreatic cancer stem cells. J. Clin. Oncol. *26*, 2806–2812.
5. Lee, H.J., You, D.D., Choi, D.W., Choi, Y.S., Kim, S.J., Won, Y.S., and Moon, H.J. (2011). Significance of CD133 as a cancer stem cell markers focusing on the tumorigenicity of pancreatic cancer cell lines. J. Korean Surg. Soc. *81*, 263–270.
6. Deshmukh, A., Deshpande, K., Arfuso, F., Newsholme, P., and Dharmarajan, A. (2016). Cancer stem cell metabolism: a potential target for cancer therapy. Mol. Cancer *15*, 69.
7. Liang, C., Qin, Y., Zhang, B., Ji, S., Shi, S., Xu, W., Liu, J., Xiang, J., Liang, D., Hu, Q., et al. (2016). Metabolic plasticity in heterogeneous pancreatic ductal adenocarcinoma. Biochim. Biophys. Acta *1866*, 177–188.
8. Lee, S.Y., Jeong, E.K., Ju, M.K., Jeon, H.M., Kim, M.Y., Kim, C.H., Park, H.G., Han, S.I., and Kang, H.S. (2017). Induction of metastasis, cancer stem cell phenotype, and oncogenic metabolism in cancer cells by ionizing radiation. Mol. Cancer *16*, 10.
9. Kim, R.K., Cui, Y.H., Yoo, K.C., Kim, I.G., Lee, M., Choi, Y.H., Suh, Y., and Lee, S.J. (2015). Radiation promotes malignant phenotypes through SRC in breast cancer cells. Cancer Sci. *106*, 78–85.
10. Levine, A.J., and Puzio-Kuter, A.M. (2010). The control of the metabolic switch in cancers by oncogenes and tumor suppressor genes. Science *330*, 1340–1344.
11. Bryant, K.L., Mancias, J.D., Kimmelman, A.C., and Der, C.J. (2014). KRAS: feeding pancreatic cancer proliferation. Trends Biochem. Sci. *39*, 91–100.
12. Hu, Y., Lu, W., Chen, G., Wang, P., Chen, Z., Zhou, Y., Ogasawara, M., Trachootham, D., Feng, L., Pelicano, H., et al. (2012). K-ras(G12V) transformation leads to mitochondrial dysfunction and a metabolic switch from oxidative phosphorylation to glycolysis. Cell Res. *22*, 399–412.
13. Yun, J., Rago, C., Cheong, I., Pagliarini, R., Angenendt, P., Rajagopalan, H., Schmidt, K., Willson, J.K., Markowitz, S., Zhou, S., et al. (2009). Glucose deprivation

contributes to the development of KRAS pathway mutations in tumor cells. Science *325*, 1555–1559.

14. Ying, H., Kimmelman, A.C., Lyssiotis, C.A., Hua, S., Chu, G.C., Fletcher-Sananikone, E., Locasale, J.W., Son, J., Zhang, H., Coloff, J.L., et al. (2012). Oncogenic Kras maintains pancreatic tumors through regulation of anabolic glucose metabolism. Cell *149*, 656–670.
15. Viale, A., Pettazzoni, P., Lyssiotis, C.A., Ying, H., Sánchez, N., Marchesini, M., Carugo, A., Green, T., Seth, S., Giuliani, V., et al. (2014). Oncogene ablation-resistant pancreatic cancer cells depend on mitochondrial function. Nature *514*, 628–632.
16. Folmes, C.D., Nelson, T.J., Dzeja, P.P., and Terzic, A. (2012). Energy metabolism plasticity enables stemness programs. Ann. N Y Acad. Sci. *1254*, 82–89.
17. Xiao, X., Su, G., Brown, S.N., Chen, L., Ren, J., and Zhao, P. (2010). Peroxisome proliferator-activated receptors gamma and alpha agonists stimulate cardiac glucose uptake via activation of AMP-activated protein kinase. J. Nutr. Biochem. *21*, 621–626.
18. Wang, Z., Wang, N., Liu, P., and Xie, X. (2016). AMPK and Cancer. Exp Suppl *107*, 203–226.
19. Donadelli, M., Costanzo, C., Beghelli, S., Scupoli, M.T., Dandrea, M., Bonora, A., Piacentini, P., Budillon, A., Caraglia, M., Scarpa, A., and Palmieri, M. (2007). Synergistic inhibition of pancreatic adenocarcinoma cell growth by trichostatin A and gemcitabine. Biochim. Biophys. Acta *1773*, 1095–1106.
20. Ju, H.Q., Gocho, T., Aguilar, M., Wu, M., Zhuang, Z.N., Fu, J., Yanaga, K., Huang, P., and Chiao, P.J. (2015). Mechanisms of Overcoming Intrinsic Resistance to Gemcitabine in Pancreatic Ductal Adenocarcinoma through the Redox Modulation. Mol. Cancer Ther. *14*, 788–798.
21. Arora, S., Bhardwaj, A., Singh, S., Srivastava, S.K., McClellan, S., Nirodi, C.S., Piazza, G.A., Grizzle, W.E., Owen, L.B., and Singh, A.P. (2013). An undesired effect of chemotherapy: gemcitabine promotes pancreatic cancer cell invasiveness through reactive oxygen species-dependent, nuclear factor κB- and hypoxia-inducible factor 1α-mediated up-regulation of CXCR4. J. Biol. Chem. *288*, 21197–21207.
22. Zhao, H., Duan, Q., Zhang, Z., Li, H., Wu, H., Shen, Q., Wang, C., and Yin, T. (2017). Up-regulation of glycolysis promotes the stemness and EMT phenotypes in gemcitabine-resistant pancreatic cancer cells. J. Cell. Mol. Med. *21*, 2055–2067.
23. Kurtoglu, M., Maher, J.C., and Lampidis, T.J. (2007). Differential toxic mechanisms of 2-deoxy-D-glucose versus 2-fluorodeoxy-D-glucose in hypoxic and normoxic tumor cells. Antioxid. Redox Signal. *9*, 1383–1390.
24. Bonnet, S., Archer, S.L., Allalunis-Turner, J., Haromy, A., Beaulieu, C., Thompson, R., Lee, C.T., Lopaschuk, G.D., Puttagunta, L., Bonnet, S., et al. (2007). A mitochondria-K+ channel axis is suppressed in cancer and its normalization promotes apoptosis and inhibits cancer growth. Cancer Cell *11*, 37–51.
25. Abel, E.V., and Simeone, D.M. (2013). Biology and clinical applications of pancreatic cancer stem cells. Gastroenterology *144*, 1241–1248.
26. Li, X., Han, G., Li, X., Kan, Q., Fan, Z., Li, Y., Ji, Y., Zhao, J., Zhang, M., Grigalavicius, M., et al. (2017). Mitochondrial pyruvate carrier function determines cell stemness and metabolic reprogramming in cancer cells. Oncotarget *8*, 46363–46380.
27. Herreros-Villanueva, M., Bujanda, L., Billadeau, D.D., and Zhang, J.S. (2014). Embryonic stem cell factors and pancreatic cancer. World J. Gastroenterol. *20*, 2247–2254.
28. Hermann, P.C., Huber, S.L., Herrler, T., Aicher, A., Ellwart, J.W., Guba, M., Bruns, C.J., and Heeschen, C. (2007). Distinct populations of cancer stem cells determine tumor growth and metastatic activity in human pancreatic cancer. Cell Stem Cell *1*, 313–323.
29. Modok, S., Mellor, H.R., and Callaghan, R. (2006). Modulation of multidrug resistance efflux pump activity to overcome chemoresistance in cancer. Curr. Opin. Pharmacol. *6*, 350–354.
30. Maruyama, H., Kleeff, J., Wildi, S., Friess, H., Büchler, M.W., Israel, M.A., and Korc, M. (1999). Id-1 and Id-2 are overexpressed in pancreatic cancer and in dysplastic lesions in chronic pancreatitis. Am. J. Pathol. *155*, 815–822.
31. Lappi-Blanco, E., Mäkinen, J.M., Lehtonen, S., Karvonen, H., Sormunen, R., Laitakari, K., Johnson, S., Mäkitaro, R., Bloigu, R., and Kaarteenaho, R. (2016). Mucin-1 correlates with survival, smoking status, and growth patterns in lung adenocarcinoma. Tumour Biol. *37*, 13811–13820.
32. Nomura, A., Banerjee, S., Chugh, R., Dudeja, V., Yamamoto, M., Vickers, S.M., and Saluja, A.K. (2015). CD133 initiates tumors, induces epithelial-mesenchymal transition and increases metastasis in pancreatic cancer. Oncotarget *6*, 8313–8322.
33. Nomura, A., Dauer, P., Gupta, V., McGinn, O., Arora, N., Majumdar, K., Uhlrich, C., 3rd, Dalluge, J., Dudeja, V., Saluja, A., and Banerjee, S. (2016). Microenvironment mediated alterations to metabolic pathways confer increased chemo-resistance in CD133+ tumor initiating cells. Oncotarget *7*, 56324–56337.
34. Long, Y.C., and Zierath, J.R. (2006). AMP-activated protein kinase signaling in metabolic regulation. J. Clin. Invest. *116*, 1776–1783.
35. Hawley, S.A., Davison, M., Woods, A., Davies, S.P., Beri, R.K., Carling, D., and Hardie, D.G. (1996). Characterization of the AMP-activated protein kinase kinase from rat liver and identification of threonine 172 as the major site at which it phosphorylates AMP-activated protein kinase. J. Biol. Chem. *271*, 27879–27887.
36. Wu, S.B., and Wei, Y.H. (2012). AMPK-mediated increase of glycolysis as an adaptive response to oxidative stress in human cells: implication of the cell survival in mitochondrial diseases. Biochim. Biophys. Acta *1822*, 233–247.
37. Yang, M., Liu, P., and Huang, P. (2016). Cancer stem cells, metabolism, and therapeutic significance. Tumour Biol. *37*, 5735–5742.
38. Schieber, M.S., and Chandel, N.S. (2013). ROS links glucose metabolism to breast cancer stem cell and EMT phenotype. Cancer Cell *23*, 265–267.
39. Zhang, D., Li, J., Wang, F., Hu, J., Wang, S., and Sun, Y. (2014). 2-Deoxy-D-glucose targeting of glucose metabolism in cancer cells as a potential therapy. Cancer Lett. *355*, 176–183.
40. Golding, J.P., Wardhaugh, T., Patrick, L., Turner, M., Phillips, J.B., Bruce, J.I., and Kimani, S.G. (2013). Targeting tumour energy metabolism potentiates the cytotoxicity of 5-aminolevulinic acid photodynamic therapy. Br. J. Cancer *109*, 976–982.
41. Raez, L.E., Papadopoulos, K., Ricart, A.D., Chiorean, E.G., Dipaola, R.S., Stein, M.N., Rocha Lima, C.M., Schlesselman, J.J., Tolba, K., Langmuir, V.K., et al. (2013). A phase I dose-escalation trial of 2-deoxy-D-glucose alone or combined with docetaxel in patients with advanced solid tumors. Cancer Chemother. Pharmacol. *71*, 523–530.
42. Yamaguchi, R., and Perkins, G. (2012). Finding a Panacea among combination cancer therapies. Cancer Res. *72*, 18–23.
43. Dwarakanath, B.S., Singh, D., Banerji, A.K., Sarin, R., Venkataramana, N.K., Jalali, R., Vishwanath, P.N., Mohanti, B.K., Tripathi, R.P., Kalia, V.K., and Jain, V. (2009). Clinical studies for improving radiotherapy with 2-deoxy-D-glucose: present status and future prospects. J. Cancer Res. Ther. *5* (*Suppl 1*), S21–S26.
44. Hanahan, D., and Weinberg, R.A. (2011). Hallmarks of cancer: the next generation. Cell *144*, 646–674.
45. Gaglio, D., Metallo, C.M., Gameiro, P.A., Hiller, K., Danna, L.S., Balestrieri, C., Alberghina, L., Stephanopoulos, G., and Chiaradonna, F. (2011). Oncogenic K-Ras decouples glucose and glutamine metabolism to support cancer cell growth. Mol. Syst. Biol. *7*, 523.
46. Roh, J.L., Park, J.Y., Kim, E.H., Jang, H.J., and Kwon, M. (2016). Activation of mitochondrial oxidation by PDK2 inhibition reverses cisplatin resistance in head and neck cancer. Cancer Lett. *371*, 20–29.
47. Dey, R., and Moraes, C.T. (2000). Lack of oxidative phosphorylation and low mitochondrial membrane potential decrease susceptibility to apoptosis and do not modulate the protective effect of Bcl-x(L) in osteosarcoma cells. J. Biol. Chem. *275*, 7087–7094.
48. Tomiyama, A., Serizawa, S., Tachibana, K., Sakurada, K., Samejima, H., Kuchino, Y., and Kitanaka, C. (2006). Critical role for mitochondrial oxidative phosphorylation in the activation of tumor suppressors Bax and Bak. J. Natl. Cancer Inst. *98*, 1462–1473.
49. Zhang, Z., Duan, Q., Zhao, H., Liu, T., Wu, H., Shen, Q., Wang, C., and Yin, T. (2016). Gemcitabine treatment promotes pancreatic cancer stemness through the Nox/ROS/NF-κB/STAT3 signaling cascade. Cancer Lett. *382*, 53–63.
50. Ushio-Fukai, M., and Rehman, J. (2014). Redox and metabolic regulation of stem/progenitor cells and their niche. Antioxid. Redox Signal. *21*, 1587–1590.
51. Kang, S.W., Lee, S., and Lee, E.K. (2015). ROS and energy metabolism in cancer cells: alliance for fast growth. Arch. Pharm. Res. *38*, 338–345.
52. Jeon, S.M., Chandel, N.S., and Hay, N. (2012). AMPK regulates NADPH homeostasis to promote tumour cell survival during energy stress. Nature *485*, 661–665.
53. Sharma, B.K., Kolhe, R., Black, S.M., Keller, J.R., Mivechi, N.F., and Satyanarayana, A. (2016). Inhibitor of differentiation 1 transcription factor promotes metabolic reprogramming in hepatocellular carcinoma cells. FASEB J. *30*, 262–275.